

Vibration control of nonlinear dynamical system via negative cubic velocity feedback

Abdullah Reda Shref^{1,*}, Yasser Amer², Mansour Nasrallah³, Osama khaled⁴,
and Eslam Sobhy⁵

¹Faculty of Artificial Intelligence, Egyptian Russian University, Cairo 11829, Egypt.

²Mathematics Department, Science Faculty, Zagazig University, Zagazig, Egypt.

³Basic Sciences Department, Higher Technological Institute, 10th of Ramadan City, Egypt.

⁴Department of Mathematical and Computer Science, Faculty of Sci. Port said University, Port Said, Egypt.

⁵Faculty of Artificial Intelligence, Egyptian Russian University, Cairo 11829, Egypt.

*Corresponding Author: Abdullah. R. E., email: Redaabdallah316@gmail.com

Received 28th December 2024, Revised 13th April 2025, Accepted 28th April 2025.

DOI: 10.21608/erurj.2025.331356.1197

ABSTRACT

The aim of this study is to highlight how specific parameters, especially nonlinear feedback control, can enhance system stability and optimize vibration control. Our findings contribute to the ongoing development of advanced strategies for managing vibrations in nonlinear dynamic systems. In this research paper, we investigate the reduction of vibrations in a hybrid Rayleigh-van der Pol-Duffing oscillator using negative cubic velocity feedback control. This system is modeled as a single-degree-of-freedom oscillator that incorporates both cubic and fifth-order nonlinear terms, along with an externally applied force. To derive a solution from the initial approximation, the multiple scales method was utilized, providing an effective analytical approach for examining the nonlinear behavior of the system. We conducted a comprehensive analysis both graphically and numerically, examining the system's behavior before and after implementing negative cubic velocity feedback, with a particular focus on the primary resonance condition ($\Omega = \omega$). MATLAB was used as the main computational tool to explore the effects of different parameters, including the impact of negative cubic velocity feedback on the primary system's response.

Keywords: Negative Cubic velocity feedback; multiple scales; Primary resonance.

1. Introduction

Many applications in engineering and physical sciences, the Duffing oscillator is one of most important models. It is utilized in optical stability, plasma oscillations, electric circuits, and buckling beams, as demonstrated by Siewe et al.(2006) and Trueba et al.(2003). Huang (2018) The Van der Pol oscillator's vibrations were suppressed using a nonlinear time-delayed feedback controller, and the impact of the feedback gain at the bifurcation point was evaluated. Amer et al. (2022) the vibration analysis and dynamic responses of a hybrid Rayleigh -Van der Pol- Duffing oscillator were studied using a proportional-derivative (PD) controller. The average method was employed to obtain the approximate solution of the vibrating system. Barron (2016) provided a numerical explanation for the behavior of a ring of coupled Van der Pol oscillators' stable and unstable responses. Barron showed that the Van der Pol oscillator's amplitude rises when the stability requirements are not satisfied. Comprehensive bifurcation investigations of the Van der Pol, Duffing, and Rayleigh oscillators were carried out by Kumar et al. (2016, 2017, and 2018), revealing and clarifying their modulating. Amer et al. (2020) two separate time delays, one for displacement and the other for velocity, were used to control the oscillator's vibrations. It was discovered that the vibrations were reduced by nearly 94% compared to their value without control, and the effectiveness of the time delay controller was approximately 17. Kandil et al. (2022) applied negative cubic velocity feedback control to manage, reduce, or stabilize a coupled pitch-roll ship model. Kamel (2009) studied multi-force stimulated coupled Van der Pol oscillators. He examined the stability of this system at two notable resonances using frequency response equations. Sayed et al.(2018) modulated the harmonic and parametric force-induced vibrations of the Van der Pol oscillator by means of negative acceleration feedback control. This simplified example demonstrates the basic steps of the Method of Multiple Scales. In the actual research (Amer et al., 2024), the system and the analysis would be more complex, involving multiple degrees of freedom, forcing terms, and potentially additional scales.

A tuned damper, or passive control, was used by Wang et al. (2018) to lessen the Van der Pol oscillator's vibrations. Through time-delay analysis, EL-Sayed (2020) demonstrated the effectiveness of positive position feedback (PPF) controllers with time delays in reducing vibrations in linked Van der Pol oscillators. Amer et al.(2020) investigated the stability of a one-degree-of-freedom Van der Pol-Duffing-Rayleigh oscillator with cubic nonlinear terms and an external force, incorporating a nonlinear integral positive position feedback controller. In order to

reduce vibrations in a vertical conveyor system, Hamed et al.(2020) used a nonlinear proportional-derivative controller (NPD). The amplitudes of two modes were reduced by roughly 95.33% and 82.45% when compared to their values prior to the use of NPD control. Amer et al. (2020) investigated the numerical and stability aspects of a hybrid Rayleigh-Van der Pol-Duffing oscillator controlled by Nonlinear Integral Positive Position Feedback (NIPPF). When Sadeghi et al. (2021) investigated the optimization of particle swarms (PSO), they found that adding more terms to the selected trial functions could reduce inaccuracy even more. In this paper, we use negative cubic velocity feedback control to suppress the vibrations of a hybrid Rayleigh-Van der Pol-Duffing oscillator excited by external forces. We solve for the one approximation of hybrid Rayleigh-Van der Pol-Duffing oscillator using the multiple scales method. We numerically modelled the behavior of the system both with and without negative cubic velocity feedback control. We used the MATLAB program to model the effects of different parameters and the negative cubic velocity on the main beam. Analytical and numerical examples are used to illustrate the effects of some selected coefficients. The convergence of the numerical and analytical solutions is proposed.

Table 1. List of symbols.

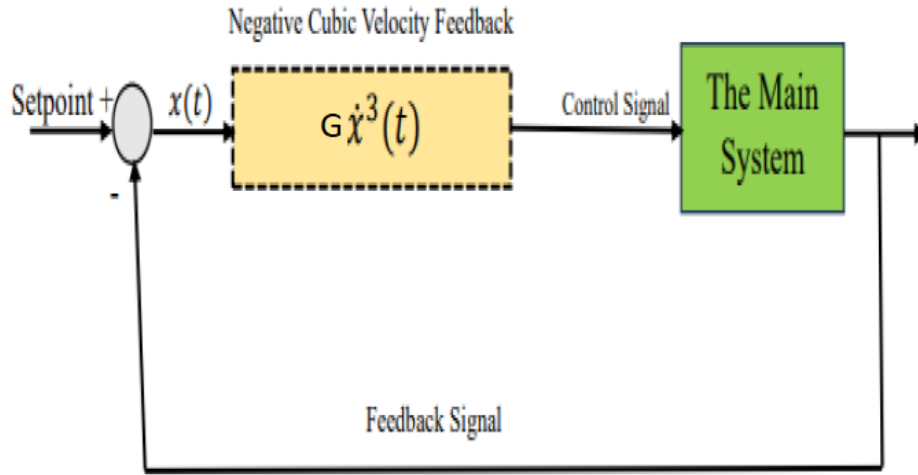
\ddot{u}, \dot{u}, u	Acceleration, velocity, and displacement of the main system respectively.
ω	The natural frequency of the main system.
Ω	The excitation frequency
μ	The damping coefficients of the main system.
$\eta, \beta, \delta, \theta, k, \lambda$	Nonlinear coefficients of the main system.
F	External excitation force is the amplitude-frequency of the external force.
G	The gain of control signal.
ε	Small perturbation parameter.

2. Mathematical modelling

A hybrid Rayleigh-Van der Pol-Duffing oscillator's one degree of freedom Nayfeh (1973):

$$\ddot{u} - 2\varepsilon\mu \left(\omega\dot{u} - \eta\dot{u}^2 - \omega\beta\dot{u}u^2 - \frac{\delta}{\omega}\dot{u}^3 - \theta\dot{u}^2u^2 \right) + 2\varepsilon\mu\omega^2 (ku^3 + \lambda u^5) + \omega^2u = 0. \tag{1}$$

To suppress the vibrations of the investigated system, the negative cubic velocity feedback controller will be used as shown in the closed-loop of the controlled system. Then Equation (1) is written as follows:



The Closed-loop control system

We reduced the vibrations of a hybrid Rayleigh-Van der Pol-Duffing oscillator by using the negative cubic velocity as follows:

$$\ddot{u} - 2\epsilon\mu \left(\omega\dot{u} - \eta\dot{u}^2 - \omega\beta\dot{u}u^2 - \frac{\delta}{\omega}\dot{u}^3 - \theta\dot{u}^2u^2 \right) + 2\epsilon\mu\omega^2 (ku^3 + \lambda u^5) + \omega^2u = \epsilon f \cos(\Omega t) - \epsilon G\dot{u}^3. \quad (2)$$

Where the position of the Hybrid Rayleigh– Van der Pol–Duffing oscillator offered by u . We used μ as the damping coefficient of the hybrid Rayleigh–Van der Pol–Duffing oscillator. The coefficients of nonlinear terms offered by $\eta, \beta, \delta, \theta, k$ and λ . The Van der Pol oscillator's frequency response is ω . The excitation's frequency and amplitude are f and Ω . The negative cubic velocity feedback indication is G .

3. The multiple scales method

Nayfeh claims (1973), for the first scale, we applied the multiple scales method. As support for this, we see that the general solution of equation (2) is

$$u(t; \epsilon) = u_o(T_o, T_1) + \epsilon u_1(T_o, T_1). \quad (3)$$

First and second derivatives use the following forms.

$$\frac{d}{dt} = D_o + \varepsilon D_1 + \dots \tag{4}$$

$$\frac{d^2}{dt^2} = D_o^2 + 2\varepsilon D_o D_1 + \dots \tag{5}$$

The derivatives $D_n = \frac{\partial}{\partial T_n}$ (n=0, 1). The first approximation solution, we conducted two time scales

$T_n = \varepsilon^n t$ where (n=0, 1). Substitute in equation (2) from (3), (4), (5) and the coefficients of the same power of ε .

$O(\varepsilon^0)$:

$$(D_o^2 + \omega^2)u_o = 0. \tag{6}$$

$O(\varepsilon)$:

$$(D_o^2 + \omega^2)u_1 = -2D_1 D_o u_o - 2\mu \left[-\omega D_o u_o + \eta (D_o u_o)^2 + \omega \beta (D_o u_o) u_o^2 + \frac{\delta}{\omega} (D_o u_o)^3 + \theta u_o^2 (D_o u_o)^2 \right] - 2\mu \omega^2 [k u_o^3 + \lambda u_o^5] + f \cos(\Omega t) - G (D_o x_o)^3 \tag{7}$$

Solve equation (6)

$$u_o(T_0, T_1) = A(T_1)e^{i\omega T_0} + \bar{A}(T_1)e^{-i\omega T_0}. \tag{8}$$

It is a homogeneous differential equation of the second order, where A is a complex function in T_1 and \bar{A} is a complex conjugate function T_1 . Substitution in equation (7) from (8).

$$(D_o^2 + \omega^2)u_1 = (-2i\omega D_1 A + 2i\mu\omega^2 A - 2i\mu\omega^2 A^2 \bar{A} - 6i\mu\delta\omega^2 A^2 \bar{A} - 6\mu k\omega^2 A^2 \bar{A} - 20\mu\lambda\omega^2 A^3 \bar{A}^2 - 3iG\omega^3 A^2 \bar{A})e^{i\omega T_0} + \frac{f}{2} e^{i\Omega T_0} + c.c \tag{9}$$

Such that $c.c$ are the complex conjugate terms.

4. The Periodic Solution

In this section, we present a detuning parameter σ to check the stability of the system in the primary resonance state as follows:

$$\Omega = \omega + \varepsilon\sigma. \tag{10}$$

Substitution in (9) of (10) and eliminating coefficients of all secular terms, yields:

$$-2i\omega D_1 A + 2i\mu\omega^2 A - 2i\mu\beta\omega^2 A^2 \bar{A} - 6i\mu\delta\omega^2 A^2 \bar{A} - 6\mu k\omega^2 A^2 \bar{A} - 20\mu\lambda\omega^2 A^3 \bar{A}^2 - 3iG\omega^3 A^2 \bar{A} + \frac{f}{2} e^{i\sigma T_1} = 0. \tag{11}$$

After converting the function A to the polar form, we have:

$$A = \frac{1}{2} a_{(T_1)} \cdot e^{i\theta_{(T_1)}}. \tag{12}$$

$$D_1 A = \frac{1}{2} (a' + ia\theta') e^{i\theta}. \tag{13}$$

Where the motion's steady state phases are θ and a. Introducing (12) and (13) in (11) and by equating the real and imaginary parts, we obtain:

$$\dot{a} = \mu\omega a - \frac{1}{4} \mu\omega(\beta + 3\delta)a^3 - \frac{3}{8} G\omega^2 a^3 + \frac{f}{2\omega} \sin \varphi. \tag{14}$$

$$a\dot{\varphi} = \sigma a - \frac{3}{4} \mu k\omega a^3 - \frac{5}{8} \mu\lambda\omega a^5 + \frac{f}{2\omega} \cos \varphi. \tag{15}$$

Where $\varphi = \sigma T_1 - \theta$.

5. Fixed-point solution

For stable-When state solution happens $\dot{a} = 0, \dot{\varphi} = 0$, the stable state solution is presented by:

$$\frac{f}{2\omega} \cos \varphi = -a\sigma + \frac{3}{4} \mu k\omega a^3 + \frac{5}{8} \mu\lambda\omega a^5. \tag{16}$$

$$\frac{f}{2\omega} \sin \varphi = -\mu\omega a + \frac{1}{4} \mu\omega(\beta + 3\delta)a^3 + \frac{3}{8} G\omega^2 a^3. \tag{17}$$

By squaring each of equations (16) and (17) and then adding, we get

$$\frac{f^2}{4\omega^2} = \left[-a\sigma + \frac{3}{4} \mu k\omega a^3 + \frac{5}{8} \mu\lambda\omega a^5 \right]^2 + \left[-\mu\omega a + \frac{1}{4} \mu\omega(\beta + 3\delta)a^3 + \frac{3}{8} G\omega^2 a^3 \right]^2. \tag{18}$$

6. Nonlinear solution

As you move to develop the stability of the steady-state solution, begin with the following:

$$a = a_0 + a_1.$$

$$\varphi = \varphi_0 + \varphi_1. \tag{19}$$

Where a_0 and φ_0 are solutions to equations (16) and (17). The disturbances a_1 and φ_1 are infinitesimal compared with a_0 and φ_0 so, substitute in Equations (14) and (15) of Equation (19)

we simply maintain the linear terms of a_0 and φ_0 . This process yields the following system:

$$\dot{a}_1 = \left[\mu\omega - \frac{3}{4}\mu\omega(\beta + 3\delta)a_0^2 - \frac{3}{4}G\omega^2a_0^2 \right] a_1 + \left[\frac{f}{2\omega} \cos \varphi_0 \right] \varphi_1 . \quad (20)$$

$$\dot{\varphi}_1 = \left[\frac{\sigma}{a_0} - \frac{9}{4}\mu k\omega a_0 - \frac{25}{8}\mu\lambda\omega a_0^3 \right] a_1 - \left[\frac{f}{2\omega a_0} \sin \varphi_0 \right] \varphi_1 . \quad (21)$$

The real part of the eigenvalues in the solution of the above system must be negative in order for it to be stable.

7. Numerical effect

We applied the MATLAB program to numerically examine the system's results. Moreover, we use the multiple scales method to examine the stability of the hybrid Rayleigh-Van der Pol–Duffing oscillator, and the effects of various parameters on the behavior of the controlled system were demonstrated. We will compare between the numerical solution and the approximate one produced by the multiple scales method. Using parametric values:

$$\omega=1 , \mu=0.01 , \eta=1.5 , \kappa=3 , \beta=1 , \delta=1/3 , \lambda=2 , f=0.5 , G=10 .$$

7.1. Time History

In order to observe the hybrid Rayleigh-Van der Pol-Duffing oscillator's behavior both before and after applying negative cubic velocity feedback control, we looked into the primary resonance situation. The time histories of the main system for the open and closed-loop designs are shown in Figures 1a and 1b. The main system's numerical differential solutions are shown by the solid red line, while the multiple scales approach's solutions are shown by the dotted blue line. The regulated system exhibited an amplitude reduction of approximately 83% in relation to the uncontrolled system. The aforementioned indicates that the control's performance (Ea the difference between the main system's stationary amplitude before and after the controller was used) is equal to 5. The convention of approximating solutions using multiple scales approach and numerical solutions using RK-4 method was also discussed from these figures. From Fig. 2 We can determine the appropriate values for the cubic velocity coefficient G where $G = 10$.

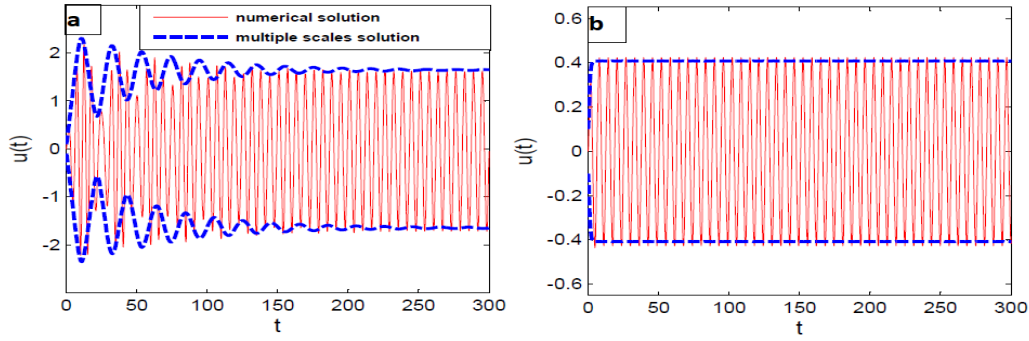


Fig. 1: The main system amplitude (a) without negative cubic velocity controller and (b) with negative cubic velocity controller.

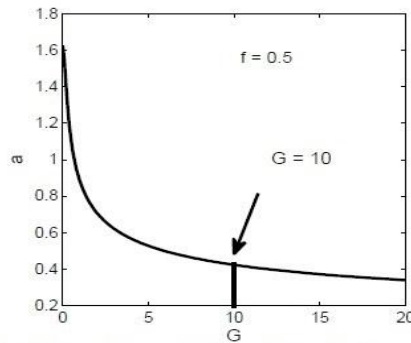


Fig.2: The effect of the cubic velocity coefficient G when $f=0.5$

7.2. Response curves

In this section, we explored the frequency response curves and the impact of the cubic velocity coefficient G , the damping coefficient μ and the excitement force f . We give the steady-state amplitude versus the detuning equation using (18) a parameter σ . From Fig. 3a in the main system, the regions of stability will increase with increasing the value of f , and the regions of stability will decrease with decreasing f . So we used negative cubic velocity controller to suppress vibrations of the main system as shown in Fig. 3b. From this figure we record down that the frequency response curve presented by one summit down by black line. The results of using RK-4 are shown by green circles. These is a perfect an agreement between two results.

The response curves of the main system a versus the detuning parameter σ is presented for $G = 10$. Such that the black line expresses the stability of the solution while the blue line expresses the instability of the solution as shown in Fig. 4a. In Fig. 4b the solution is stable for large values of G and the main system's amplitude is monotonic decreasing function on the negative Cubic velocity feedback coefficient G the solution is stable for large values of G While the stability region

decreases at small values. For the external force, the main system's amplitude is monotonic decreasing function and the solution is stable for large values of f as exhibit in Fig. 4c. The amplitude increasing for small values of the natural frequency ω the solution is stable for little values of ω as seen in Fig. 4d.

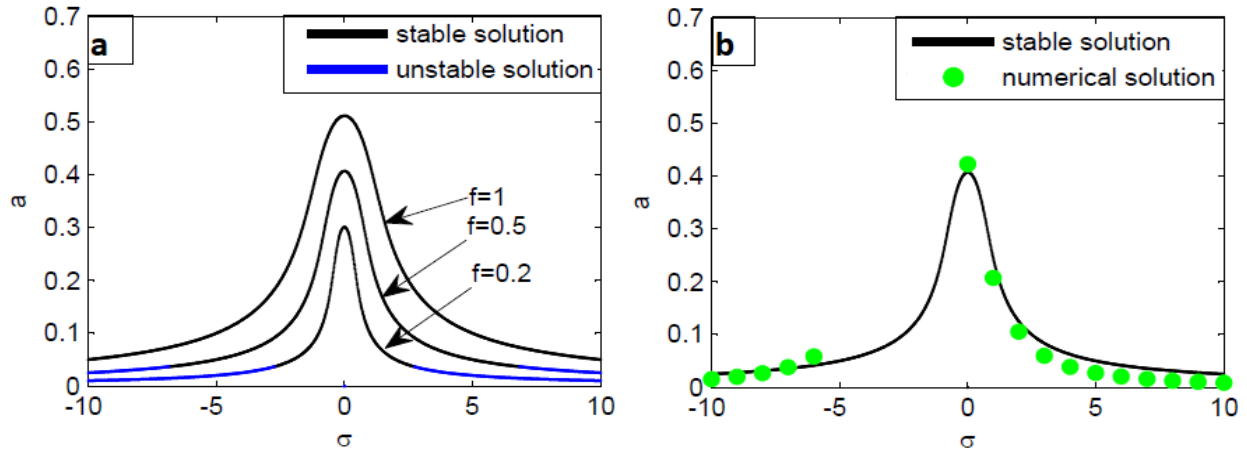
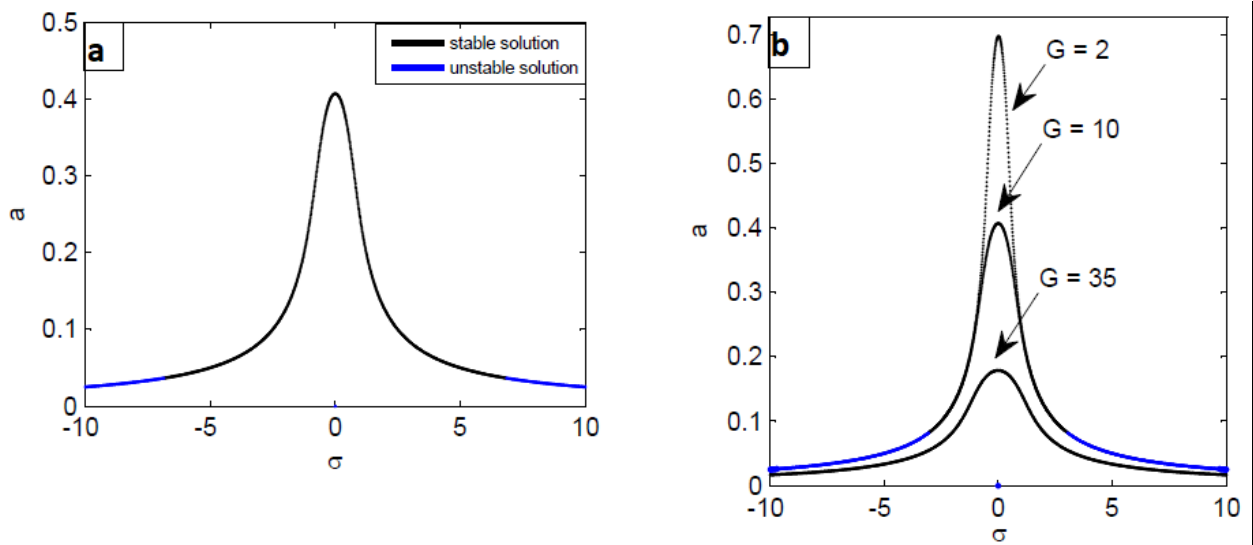


Fig. 3: (a) impact the external force without control (b) the response curve after control.



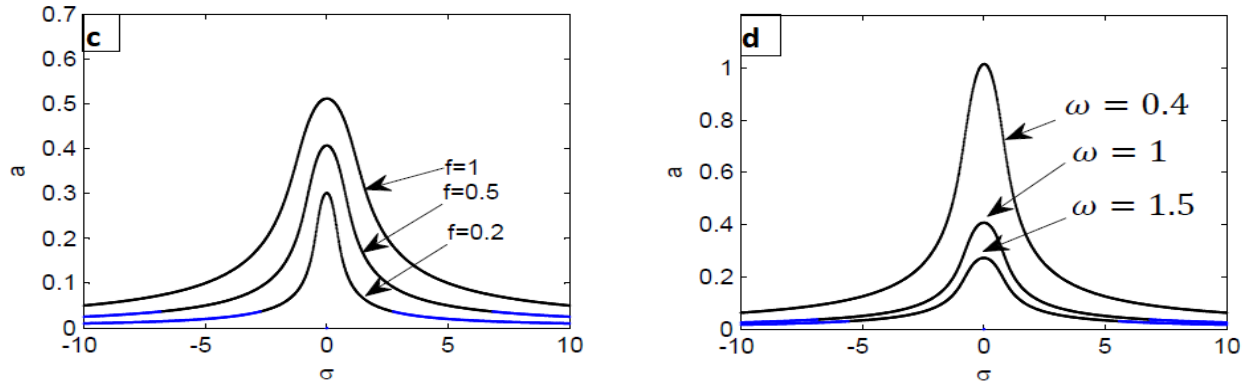


Fig. 4: (a) the response curves of the controlled system where $G = 10$. (b) The response curves for different values of cubic velocity coefficient G . (c) The external force action. (d) The natural frequency ω action.

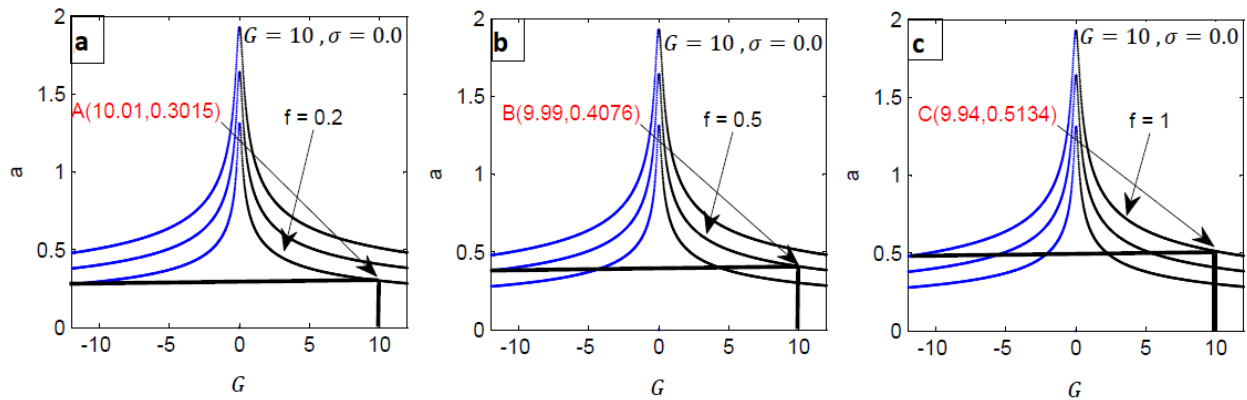


Fig. 5: (a), (b) and (c) They show cubic velocity coefficient G at different values for such that $f \sigma = 0$

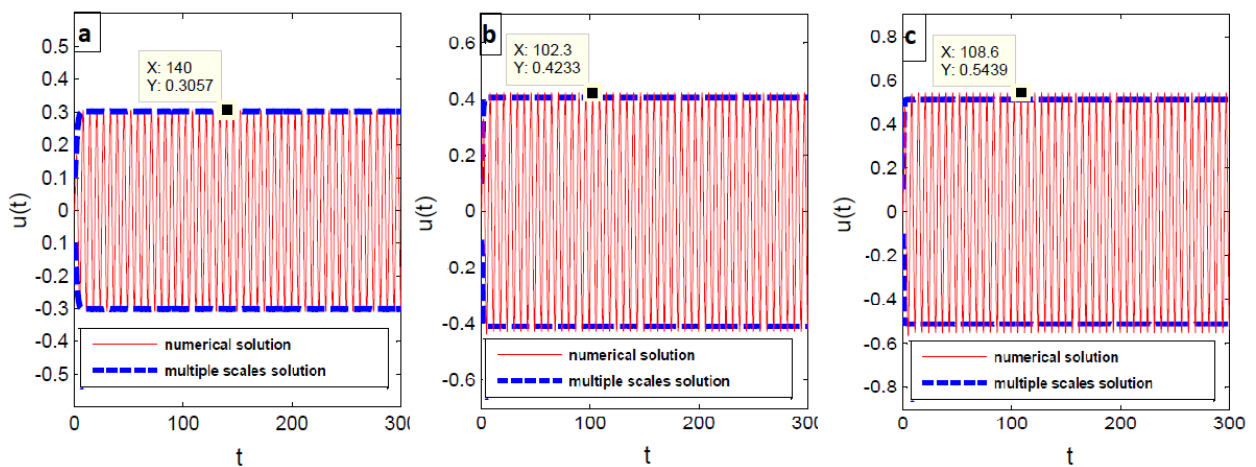


Fig. 6: The time histories of the main system for different values for f such that $\sigma = 0$. (a) corresponds to point A in Fig. 5a and (b) corresponds to point B in Fig. 5b and (c) corresponds to point C in Fig. 5c.

Fig. 5, 6: present the time-domain responses of the primary system under three distinct parameter settings, corresponding to the representative operating points A, B, and C identified in the previous analysis.

(a) The first plot illustrates the system's dynamic behavior at operating point A. The simulation covers a duration of 300 time units, where the blue curve represents the numerical integration results, and the red curve corresponds to the approximate analytical solution derived using the method of multiple scales.

(b) The second plot shows the time response at point B, using a different set of parameter values. As before, both the numerical and analytical solutions are displayed for comparison over the same time interval.

(c) The third plot corresponds to point C, capturing the system's temporal evolution under another parameter configuration. The alignment between the numerical and analytical solutions over the 300 time-unit span further validates the effectiveness of the adopted analytical approach.

These time history plots provide a visual representation of the system's response for the specific parameter values indicated by the corresponding points in the previous figures. The comparison between the numerical solution and the multiple scales solution allows for an assessment of the accuracy of the approximation methods used.

From these physical interpretations, we can observe how the values of the cubic velocity coefficient parameters G and σ affect the stability and temporal behavior of the system.

The key points are: We notice that the values match between images fig. 5 and fig. 6, and this indicates the efficiency of the negative cubic velocity feedback control. The time history plots visualize the system's response for specific parameter values. Comparing the numerical and multiple scales solutions allows for evaluating the accuracy of the approximation methods. The increase in G and σ values causes the system to transition from linear to nonlinear and chaotic temporal behavior, highlighting the critical role of these parameters in determining the system's stability and dynamics.

8. Conclusion

The oscillator is one of the most important models in physics and engineering, where the Duffing equation finds many uses. Examined were the Van der Pol – Duffing – Rayleigh oscillator's dynamic responses and vibration analysis when subjected to an external force. We employed the multiple scales approach to get the vibrating system's approximate solution. To reduce the hybrid Rayleigh-van der Pol-Duffing oscillator's large amplitudes, the negative Cubic velocity control feedback was incorporated. The negative cubic velocity feedback control was added to decrease the high amplitudes of the hybrid Rayleigh–van der Pol–Duffing oscillator. The analytical solution up to first-order approximation is obtained by using the method of multiple scales. In comparison to the uncontrolled system, the controlled system's amplitude was reduced by about 83%. This means that the control E_a performance is about 5. From this research we will present some important outputs for the influence of the vibrating system's parameter such that:

- i. The amplitude of the system increases as the external forces acting increase.
- ii. The amplitude of controlled system decreases as the cubic velocity coefficient G increases and the solution is stable at large values.
- iii. The amplitude of the system decreases with decreasing value of the natural frequency ω .
- iv. The response curves, the FRC Solution and RK-4 Solution have a good agreement.

Declaration of conflicting interests

The author(s) declared no potential conflicts of interest with respect to the research, authorship, and/or publication of this article.

Funding Statement:

The authors received no specific funding for this study.

9. References

- 1) Amer, Y. A., Abd EL-Salam, M. N., & EL-Sayed, M. A. (2022). Behavior of a Hybrid Rayleigh-Van der Pol-Duffing Oscillator with a PD Controller. *Journal of applied research and technology*, 20(1), 58-67.
- 2) Amer, Y. A., El-Sayed, A. T., & Abd EL-Salam, M. N. (2020). Position and Velocity Time Delay for Suppression Vibrations of a Hybrid Ray-leigh-Van der Pol-Duffing Oscillator. *Sound & Vibration*, 54(3), 149-161.
- 3) Kandil, A., Hamed, Y. S., Abualnaja, K. M., Awrejcewicz, J., & Bednarek, M. (2022). 1/3 Order Subharmonic Resonance Control of a Mass-Damper-Spring Model via Cubic-Position Negative-Velocity Feedback. *Symmetry*, 14(4), 685.
- 4) Amer, Y. A., El-Sayed, A. T., & Abd EL-Salam, M. N. (2020). Outcomes of the NIPPF Controller Linked to a Hybrid Rayleigh–Van der Pol-Duffing Oscillator. *Journal of Control Engineering and Applied Informatics*, 22(3), 33-41.
- 5) Barron M. A. (2016). Stability of a ring of coupled van der Pol oscillators with non-uniform distribution of the coupling parameter. *Journal of Applied Research and Technology* 14(1), 62-66.
- 6) EL-Sayed, A. T. (2020). Resonance behavior in coupled Van der Pol harmonic oscillators with controllers and delayed feedback. *Journal of Vibration and Control*, 27(9-10), 1155-1170.
- 7) Hamed, Y. S., Alotaibi, H., & El-Zahar, E. R. (2020). Nonlinear Vibrations Analysis and Dynamic Responses of a Vertical Conveyor System Controlled by a Proportional Derivative Controller. *IEEE Access* 8, 119082-119093.
- 8) Kumar, P., Kumar, A., Racic, V., & Erlicher, S. (2018). Modelling vertical human walking forces using self-sustained oscilla-tor. *Mechanical Systems and Signal Processing*, 99, 345-363.
- 9) Kumar, P., Kumar, A., & Erlicher, S. (2017). A modified hybrid Van der Pol–Duffing–Rayleigh oscillator for modelling the lateral walking force on a rigid floor. *Physica D: Nonlinear Phenomena*, 358, 1-14.
- 10) Kumar, P., Narayanan, S., & Gupta, S. (2016) Investigations on the bifurcation of a noisy Duffing–van der Pol oscillator. *Probabilistic Engineering Mechanics*, 45, 70-86.
- 11) Huang C (2018) Multiple scales scheme for bifurcation in a delayed extended van der Pol oscillator. *Physica A: Statistical Mechanics and its Applications*, 490, 643-652.
- 12) Sayed, M., Elagan, S. K., Higazy, M., & Abd Elgafoor, M. S. (2018). Feedback control and stability of the Van der Pol equation subjected to external and parametric excitation forces. *International Journal of Applied Engineering Research*, 13(6), 3772-3783.
- 13) Amer, Y.A., Abdullah, R.E., khaled, O.M. et al. Vibration Control of Smooth and Discontinuous Oscillator via Negative Derivative Feedback. *J. Vib. Eng. Technol.* (2024).
- 14) Siewe, M. S., Kakmeni, F. M., Bowong, S., & Tchawoua, C. (2006). Non-linear response of a self-sustained electromechanical seismo-graphs to fifth resonance excitations and chaos control. *Chaos, Solitons & Fractals*, 29(2), 431-445.
- 15) Trueba, J. L., Baltanás, J. P., & Sanjuán, M. A. (2003). A generalized perturbed pendulum. *Chaos, Solitons & Fractals*, 15(5), 911-924.
- 16) Sadeghi, S. A. M., Ebrahimpour, B., Bakhshinezhad, N., & Sadeghi, S. M. N. M. M. (2021). Analytical solution of nonlinear Van der Pol oscillator using a hybrid intelligent

- analytical inverse method. *Turkish Journal of Computer and Mathematics Education (TURCOMAT)*, 12(13), 5614-5625.
- 17) Kamel, M. M. (2009). Nonlinear behavior of Van der Pol oscillators under parametric and harmonic excitations. *Physica Scripta*, 79(2), 025004.
 - 18) Wang, W., Wang, X., Hua, X., Song, G., & Chen, Z. (2018). Vibration control of vortex-induced vibrations of a bridge deck by a single-side pounding tuned mass damper. *Engineering Structures*, 173, 61-75.
 - 19) Nayfeh AH (1973) *Perturbation Methods*. New York: John Wiley & Sons.